Evolution of Au(111) electrode surface in different electrolytes and conditions studied with a home-made EC-STM

Behjati, S.

Chapter 2

Electrochemical Scanning Tunneling Microscope (EC-STM)

This chapter consists of two sections. Section 2.1 introduces the basic working principle of a Scanning Tunneling Microscope (STM). After familiarizing with STM, section 2.2 describes the design of the Electrochemical STM (EC-STM) and the main modules used for the work described in the rest of the thesis.

2.1 Scanning Tunneling Microscope

Binning and Rohrer invented the first Scanning Tunneling Microscope (STM) in 1981 [10, 11], which for the first time allowed surface scientists to directly image the real spatial structural and electronic properties of their surfaces. Depending on the type of experiment, STM can be done on surfaces in vacuum, air, or a liquid. An additional possibility is to perform so-called scanning tunneling spectroscopy, which gives information about the density of electrons as a function of their energy[12, 13]. It also can be used to manipulate and reposition the atoms[14]. After the emergence of STM, other scanning probe techniques like atomic force microscopy (AFM) were developed. The operation of STM relies on electron tunneling, a quantum mechanical phenomenon enabling electrons to tunnel through an insulating barrier between two electrodes. As a result of the applied bias potential V_{Bias} to the electrodes, tunneling can take place and the corresponding tunneling current I_t can be measured by a proper amplifier. This tunneling current is a function of the distance between the electrodes, the tunneling bias potential, and the density of states (DOS) of the electrodes. Thereby, it contains information about the electrode distance and the electronic structure of both electrodes[15].

Figure 2.1 shows the working principle of a scanning tunneling microscope. An atomically sharp metallic tip (first electrode) is positioned close to the conductive or semi-conductive sample (second electrode). If the tip-sample distance is reduced to a few Å, the tip and the sample wave functions overlap. If a bias potential is applied at this condition, the electrons can tunnel from the tip to the sample or vice versa, depending on the sign of the applied potential. The majority of the tunneling current occurs through the atoms at the apex of the tip, primarily due to its exponential dependence on the tip-sample distance. This results in a distinct localization of the tunneling current and, as a consequence, contributes to the high-resolution capabilities of the STM. The tip is mounted on a piezoelectric tube which allows very precise movement of the tip in 3 dimensions. Via the piezoelectric effect, precise movement of the tip is easy to achieve. During the measurement, the tip can move in the X-Y plane to scan the area under study and the z-axis can be used to measure or control the tip-sample distance. There are two main working modes for STM: namely constant current mode and constant height mode, of which the first one is used most frequently. In the constant current mode, the tunneling current is being monitored as a function of the X-Y position of the tip and by using feedback, the tunneling current will be kept constant by applying changes in the tip height. Thus, by recording the displacement of the tip in the z-axis as a function of the X-Y position, one can extract the topography of the sample surface with atomic resolution. The tunneling current in STM is typically quite low, ranging from 0.01 to 50 nA. Consequently, the current amplifier plays a crucial role in the STM functionality by magnifying this small tunneling current and transforming it into a measurable voltage, because for the feedback system or the main controller voltage level that tiny current is not useful. The characteristics of the current amplifier significantly impact the overall performance of the STM, which is influenced by factors such as thermal noise, stray capacitance, and the inherent characteristics of electronic components. The next required part is the controller which generates the scanning signals of the piezo tube and it usually contains a logarithmic amplifier and a PID controller to adjust the height of the tip during the scans. The controller typically can be connected to a PC to gather the information and plot the images. Since the working voltage range of the piezoelectric tube is much higher than the working voltage

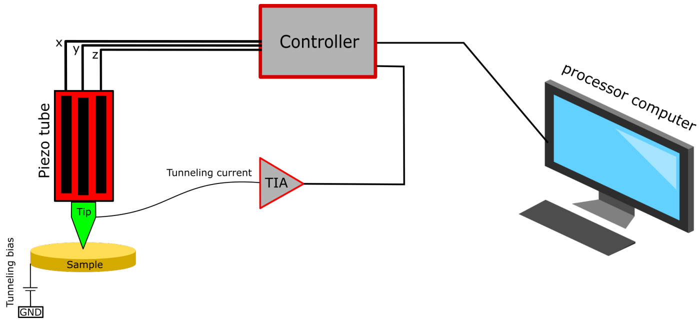

Figure 2.1: Working principle of an STM. The applied potential to the piezoelectric tube can move the tip in three dimensions and the change in current on the tip which can be measured by a transimpedance amplifier (TIA), can provide the input for the feedback signal to adjust the tip-sample distance (constant current mode) or a signal to calculate the distance between the tip and the sample (constant height mode).

of the controller, an extra-high-voltage amplifier is essential to multiply the low-level output voltage of the controller by a constant coefficient. There are many different types of mechanical designs for an STM like, single-tube STM, the beetle, the walker, and many others[15]. Each design has its own strong and weak points and it can be chosen for the specific aim of the research. Among them, single-tube is the most common because of its small size and high natural resonance frequency which makes the mechanical design and vibration isolation system simpler. In this design, the piezo scanner tube is fixed to the central portion of a robust and rather heavy metal cylinder. The tip can be mounted on the apex of the piezoelectric element. This metal cylinder, including the piezoelectric element, is called the scanning head. The head can be mounted on three screws with polished spherical ends, and the screws should be fixed on the base plate where the sample is securely fixed. Two screws can be used for coarse approaching steps to move the tip very close to the sample surface. Subsequently, precise positioning can be achieved by controlling the third screw for fine adjustments. Typically, a step motor drives the screw and helps to deploy automatic approach procedures.

2.2 Electrochemical Scanning Tunneling Microscope

The working principle of a scanning tunneling microscope and regular electrochemical experiment in an EC cell has been discussed in the previous two sections. For an in-situ scanning tunneling microscope for electrochemistry, combining a normal STM and EC experiment setup is desirable. By achieving this goal, one can study the sample topography of the electrode surface on a specific spot with atomic resolution before, during, and after electrochemical experiments. A simple schematic of this setup is shown in Figure 2.2. The scanner head (piezoelectric tube), SPM controller, and processing PC are the main parts of the STM setup, and by adding potentiostat, electrochemical cell, and electrodes, an EC-STM can be built. To integrate an STM with an EC setup, multiple electrical modules with specific characteristics, mechanical parts, and software are necessary. In the following sections, these subjects will be covered.

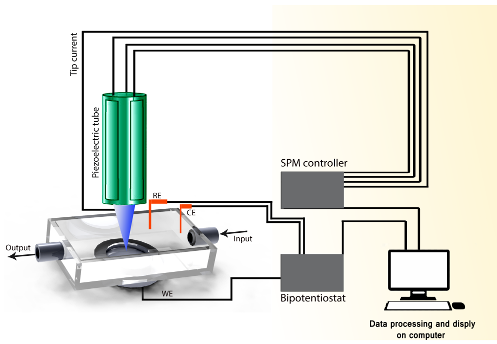

Figure 2.2: Simple schematics of an Electrochemical Scanning Tunneling Microscope (EC-STM).

2.2.1 Potentiostat for EC-STM

The reason for having a potentiostat in a normal electrochemical experiment was discussed in section 1.1. Since the scanning probe (tip) as an extra electrode is needed for an EC-STM, an additional requirement is essential for the potentiostat. The primary extra capability is the ability to independently adjust or tune the working electrode voltage with respect to the tip. In conventional electrochemical experiments, the voltage difference between the working electrode and the reference electrode is important while the voltage of the working electrode has no importance by itself and it can be grounded or remains float. However in an EC-STM, since a voltage difference (tunneling bias) is needed, we must be able to control the WE potential separately so that it does not interfere with the applied electrochemical potential. There are different types of potentiostat with various working principles and thus a comparison is inevitable for making a decision for the EC-STM potentiostat. In the following section, the three main categories will be brought up.

Resistive-Based Potentiostat

The first type and the most common type of potentiostat contains a resistor and operational amplifier to control the voltage difference between the working electrode and the reference electrode and measure the current flowing through the electrochemical cell. Because of the circuit configuration, the current passing through the working electrode has to pass through the resistor R and this will make a voltage difference at the output of the operational amplifier which has a linear correlation with the current and this is called transimpedance amplifier. The formula for the output can be written as:

$$V_{\text{out}} = -I_{\text{EC}} \times R \tag{2.1}$$

where V_{out} is the output voltage and I_{EC} is the electrochemical current in the cell. The simple schematic of this configuration is shown in Figure 2.3. It is also possible to implement the transimpedance amplifier on the counter electrode since the current passing through the working electrode is theoretically equal to the current at the counter electrode if we consider the current at the reference electrode negligible. However, doing so can increase the complexity and noise level of the system since more active components will be needed for the entire potentiostat configuration. Furthermore, stability issues may arise as the transimpedance amplifier is integrated within the primary feedback loop. A weak point to be considered for this configuration is its inefficiency for the experiments that need high current because the power in the resistor R in Figure 2.3 will turn into heat. Considering the formula for the electrical power loss in a resistor as $P = RI^2$ where I is the electrochemical current passing through the EC cell, this reduces the efficiency of this circuit. Lower R values result in lower power loss but reduce the current reading precision. Thus, there is a trade-off between the electrical power loss and the current reading precision. However, the precision and frequency response of this configuration are satisfactory.

The other approach can be placing a resistor in series in the path of either the counter electrode or working electrode. In the case of the former, the working electrode should be connected to the ground with a resistor R in series. The passing current will make a voltage difference and this voltage can be measured by a voltage follower. However, it is important to note that this voltage difference will also alter the working electrode voltage, which is not desirable. In other words, the WE voltage will become a function of the EC current. To compensate for this unwanted effect, an extra circuit

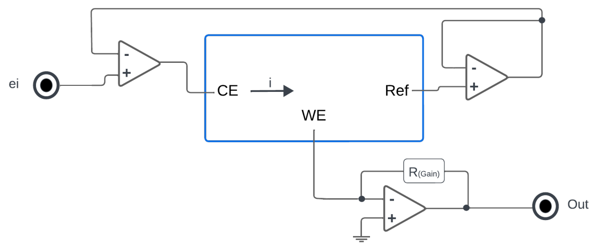

Figure 2.3: Resistor-based potentiostat schematic containing a resistor and operational amplifier.

is needed. In brief, the main issue with this approach can be the lack of enough precision for very small currents. There is a trade-off between the precision and the voltage difference introduced into the measurement.

Capacitive-based Potentiostat

An alternative approach is using a capacitor in the current sensing circuit, instead of a resistor. It is well known that the voltage across a capacitor is equal to the integrated current passing through the capacitor over time. Thus by reading the capacitor voltage one can calculate the total current passing through. As shown in Figure 2.4, it is essential to discharge the capacitor to avoid current blockage in the case of a fully charged capacitor. Thus, a transistor or CMOS switch will be turned on if the capacitor's voltage reaches a certain voltage threshold. The frequency of the applied pulses to the switch can be a proper parameter for current calculation. This technique can be used in either the working electrode or the counter electrode. This method is capable of increasing the efficiency of the potentiostat (the ratio of the electrical energy used in the electrochemical cell to the total energy consumed by the potentiostat). Thus, it is more favorable for high current measurement. Another advantage is the capability to measure different current ranges without the need for changing the capacitor. By contrast, for the aforementioned method of resistor-based potentiostat, changing the resistor is essential. For very high-accuracy experiments with this configuration, one can use a delta-sigma modulator as a recovery module[16]. The shortcoming of this method can be the leakage current in the capacitor and more importantly, the applied pulses on the switch can impose some noise into the electrochemical system.

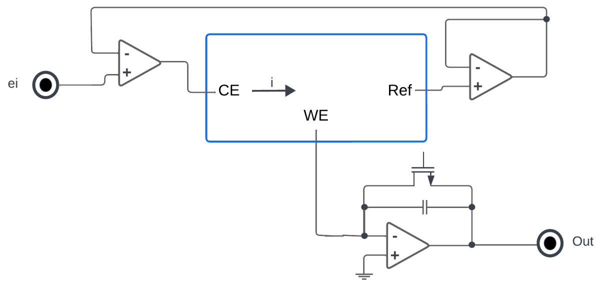

Figure 2.4: Capacitor-based current sensing circuit.

Current Mirror-Based Potentiostat

To enhance stability and mitigate the impact of discharging pulses on the potentiostat system, a current mirror method can be used which is shown in Figure 2.5. In this method, by the proper components, a mirrored current of the either working electrode or counter electrode is made and this current can be measured by a transimpedance amplifier configuration or capacitive-based current sensing. By implementing this method, the current sensing system and the main electrochemical current will be separated and the current sensing circuit will not be able to disturb the performance.

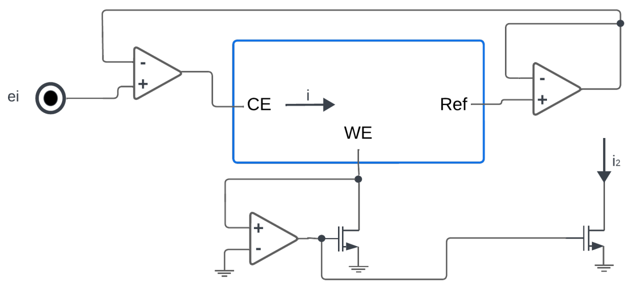

Figure 2.5: Current mirror method for current measurement in a potentiostat.

Schematics and working principle of the potentiostat

Between the three aforementioned modes, the resistor-based potentiostat seems the best fit for an EC-STM for the following reasons: First, the surface area of the sample under study is a few squared millimeters, thus the magnitude of current will be from nano ampere to a few milli-ampere range. Thus, the energy loss of the resistor in the transimpedance configuration can be negligible. Second, this method does not add extra noise (like noise coming from pulses on the switch) to the experiments, and avoiding noise is crucial in an EC-STM. Finally, this configuration allows a fine control of the working electrode potential without affecting the EC potential which is crucial for an EC-STM.

Figure 2.6 shows the schematics of the designed potentiostat. On the left-hand side, four inputs are shown. The two top inputs will set the electrochemical voltage and can accept two AC and DC signals. The DC input is suitable for a low-speed changing waveform, like a conventional triangular waveform for a cyclic voltammogram. The AC input can be used for other fast-changing signals and it helps to deploy ACV techniques. The two bottom inputs can adjust the working electrode potential, which in a conventional potentiostat is either grounded or remains floating. With this configuration, the WE potential can be adjusted precisely by a DC voltage or with an AC potential to apply modulation techniques to the tunneling bias. All the inputs are passed by a second-order active low pass filter to reduce the unwanted noises at the inputs. The working electrode is connected to a transimpedance amplifier to convert the current on the WE into a readable voltage which can be read at WE I_{Out} connector. There are seven different current ranges available and can be changed digitally from $1\mu A$ to $200mA$. With $1\mu A$ as the current range setting, nano ampere currents can be read. These gain settings can also influence the bandwidth and phase margin of the potentiostat. As a rule of thumb, higher transimpedance gains will cause a reduction in the bandwidth. Another operational amplifier with a voltage follower configuration is connected to the WE to read the actual voltage. This is important because the bandwidth limitations and wrong gain settings can lead to strong deviation from the asked WE potential. To improve the reliability and precision of the potentiostat the WE potential is always read directly by the circuit. This voltage is detectable at the WE U_{Out} connector. The reference electrode is directly connected to the non-inverting input of the operational amplifier with a voltage follower configuration. This makes reading of the Ref potential possible with great precision and the output is connected to Ref U_{Out}. The final part is the counter electrode driver module which reads the EC potential setpoint from the active filter output, the reference electrode voltage, and the actual working electrode potential to adjust the counter electrode voltage so that the voltage difference between the working electrode and the reference electrode matches with the asked EC potential. The bandwidth of this module is adjustable with four digitally controlled channels. The main specification of the designed potentiostat is as follows:

- Tunable bandwidth for CE.
- Tunable bandwidth and gain for WE.
- Maximum 5 picoampere RE input current (very low ohmic error).
- Second-order low-pass active filter on inputs.
- AC and DC inputs for each channel (AC for modulation and DC for voltage sweep).
- 200 mA continuous output current.
- Control of CMOS switches with 10 ns resolution.
- Everything is controlled by the *FPGA* (no selector or knob) and the instrument can be run remotely.

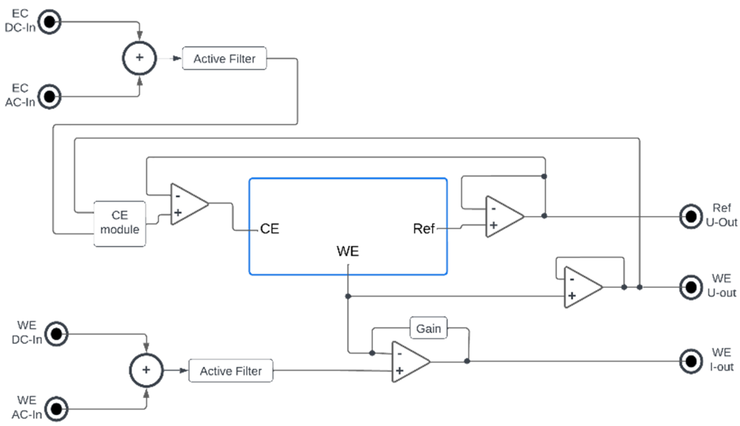

Figure 2.6: Simple schematics of the potentiostat with the cell containing the electrodes in the middle. On the left, there are four input channels, and on the right, three outputs are shown.

After finishing the schematic design, the printed circuit board, which is shown in Figures 2.7a (upper side) and 2.7b (lower side), was developed. Figure 2.7c shows the final product with a metallic box to reduce the electromagnetic noise during the precise experiments. There is one National Instrument DAQ card on the right side of the potentiostat which contains four digital-to-analog converters and four analog-to-digital converters with 16 bits resolution. Thus, all the waveform can be generated by this module and be passed to the potentiostat and all the output voltages from the potentiostat can be read by the DAQ card. Home-built software is needed to run electrochemical experiments with different techniques, which will be discussed in the next section.

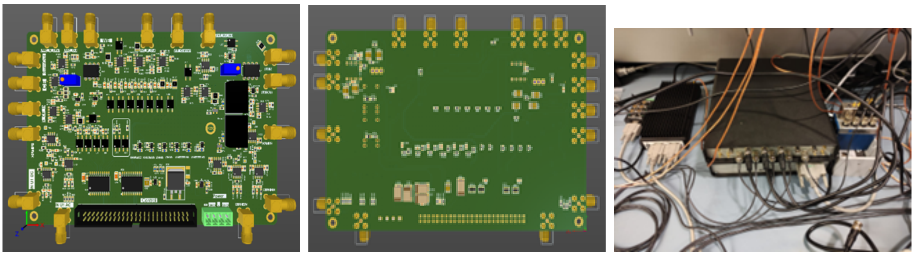

(a) (b) (c)

Figure 2.7: The designed printed circuit board top and bottom (a and b) and the final module in a metallic box (c).

The potentiostat software

As was explained in the previous section, the potentiostat is connected to a NI DAQ card, and a home-built software was developed to facilitate the generation of the working electrode and other voltages and read, process, plot, and save the measured signals. The basic version of the software contains two fundamental techniques for electrochemistry experiments, namely chronoamperometry and cyclic voltammetry. Figure 2.8 depicts the window for the chronoamperometry and basic potentiostat settings like the gains and bandwidth. On the top left-hand side, the CA technique can be started and stopped by run and stop buttons, respectively. Below these buttons, the working electrode potential and the electrochemical potential can be set by the operator and those voltages will be applied immediately while the software is running. There is a cluster containing four boxes where it shows the value of the working electrode potential (tunneling bias voltage), electrochemical voltage, electrochemical current on WE, and current on the tip. On the bottom, the real-time plot can be screened during the experiment. On the top right-hand side, There is a window for adjusting the settings, such as turning the potentiostat into an open circuit configuration, adjusting the counter electrode bandwidth, and working electrode transimpedance gain and bandwidth. This window is usually used to start many conventional EC experiments since the first step can be closing the circuit and applying a voltage (usually in the double-layer potential window).

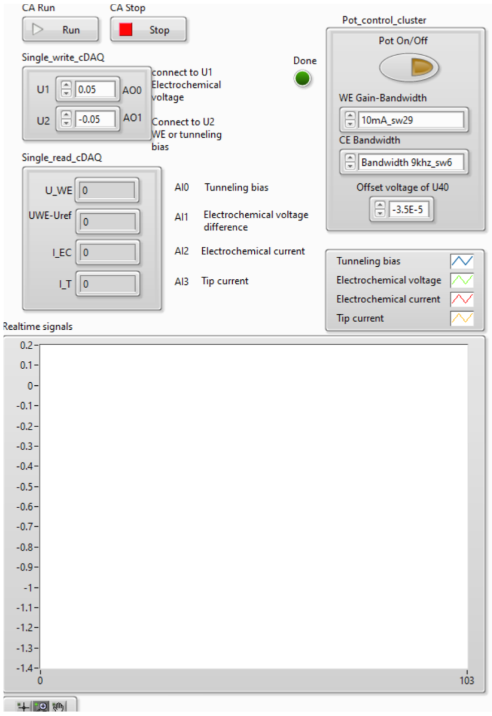

Figure 2.8: Chronoamperometry window of the potentiostat software

The next window in Figure 2.9 is designed for measuring a cyclic voltammogram or applying a voltage sweep from a certain voltage to either higher or lower potential. On the left-hand side, the operator can change the start potential for the CV, vertex one and vertex two, end potential, scan rate in volts per second, number of scans that need to be applied, tunneling bias voltage during the cycles, and oversampling factor. The parameters are self-explanatory except the last one. Over over-sampling factor tells the software how many data points need to be recorded on all the inputs for each applied data point on the output (WE and EC potential during the CV and LVS experiments). By elevating this value, a greater number of data points can be captured, potentially allowing for the reduction of inherent electrical noise through methods such as averaging over-sampled data points or implementing digital filters. After adjusting all the items, the run button can be pressed and the CV will be recorded and plotted in real-time on the large window. The recorded data can be automatically saved with the description and experiment name on the hard drive for further analysis.

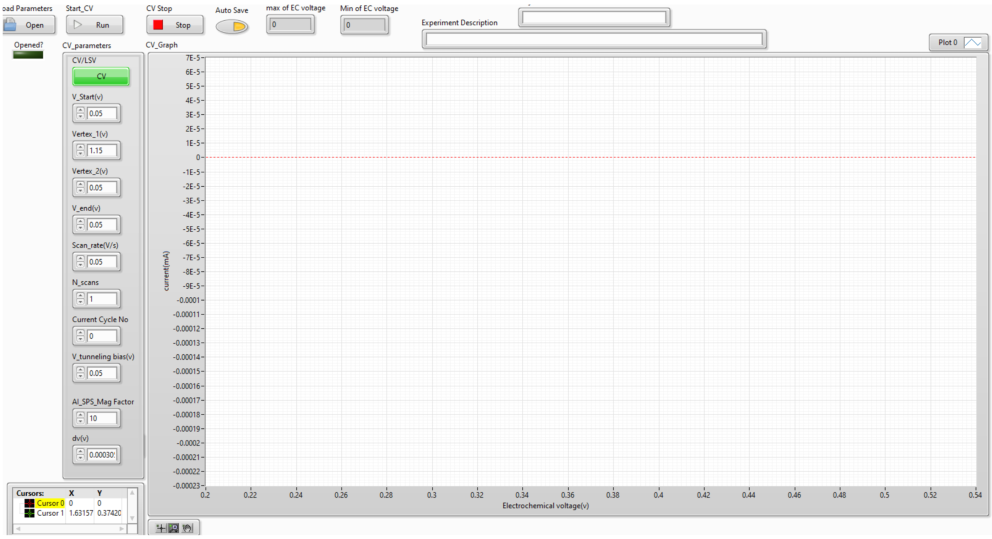

Figure 2.9: Cyclic voltammogram window of the potentiostat software.

To make sure the potentiostat (the electronics and the software) is working flawlessly, a 10 kΩ resistor and a 0.1 µF capacitor were connected separately between the WE and CE, and the reference electrode was connected to the CE. Then a cyclic voltammogram was recorded to test the performance under capacitive and resistive loads. The observed outcomes aligned with expectations.

2.2.2 Controller

The other essential module is the controller which should be able to perform many tasks. First, the controller generates scanning waveforms for the x and y piezoelectric elements. These waveforms contain one fast-changing triangular waveform for movement in the X direction and one slow-moving waveform for the Y direction. For each complete triangle, the tip will move in the X direction, reach the maximum distance, and then come back to the original starting point. By applying a very slow changing voltage sweep (or triangular waveform in case of scanning upward and downward continuously) the tip location in the Y axis will be modified. There are many parameters for these waveforms that the controller must be able to modify like frequency of the triangular waveform, voltage magnitude for the waveform, and offset potential for X and Y signal. Second, the height of the tip needs to be adjusted based on the tunneling current on the tip. Therefore, a feedback signal needs to be generated to keep the tip current as close as the set current setpoint. It can be done by PID controller and it can be implemented inside the SPM controllers. Thus, the controller will generate the feedback signal to control the height of the tip and it also records the values for each data point. Finally, by having the feedback signal value along with the X-Y waveform data, the controller can generate and plot the topographical image of the scanned surface. This task can be done in the controller software installed on a PC. It is important to keep in mind that there are many more technical functionalities for modern SPM controllers that we did not discuss in this section. Commercial SPM controllers are available nowadays and they can match the requirements of many projects. For many reasons, open-source software for the controller is very useful since each instrument needs specific modifications in the software for a smooth operation. For instance, for the coarse approach mechanism, the controller should communicate with the actuator's module, and having access to the source code is very helpful in modifying the software. Thus, MK3 controller from Soft dB company, as shown in Figure 2.10, was purchased and used. There are controllers with better precision, speed, and more sophisticated electronics but considering the price and having no access to the source code, could prevent us from employing them for this instrument. There are eight inputs and eight outputs with 16 bits of precision on this controller. The channels can be assigned to different input and output signals.

Figure 2.10: Open-Source SPM Controller, Model MK3.

2.2.3 Analog Module

The analog module was designed and manufactured to take care of all the analog operations on the input and output signals. This module has two main parts and each part has its sub-modules. The first part is called "XYZ modules" and is for all the analog operations on control signals for the piezoelectric in the X, Y, and Z axis. The second part is related to the generation of control signals and some necessary arithmetic operations on the tunneling current signal. These two parts will be discussed in more detail in the following.

X, Y, and Z modules

The controlling signals for X, Y, and Z can be made in the main controller but more essential operations are needed. First, since the controller is capable of generating signals from -10 to + 10 volts with 16 bits precision, in some experiments it is required to reduce the voltage span to increase in precision further. One application for this operation is precision improvement for small scan areas and atomically flat surfaces. In this case, the instrument should have a very high resolution in the X, Y, and Z directions. This can be achieved by division of the signals by a certain coefficient. Second, in the case that one wants to zoom in on a small area (compared to the total travel range of the piezoelectric tube), it is important to separate the scanning signal and the offset signal. By applying this, one can record high-precision pictures on a small area while having access to the whole travel range of the piezoelectric tube. The offset signal is also useful for compensating the thermal drifts in all three directions during long experiments. Moreover, in some cases, one needs to apply some modulation in different directions with a certain frequency. So, external modulation signals need to be added to the offset and scanning signals. Third, the out-of-range potential of the piezo is damaging and needs to be avoided. Since commercial high-voltage amplifiers usually have a fixed gain value, it is wise to have good control on the output voltage levels. Fourth, a high order low pass filter can reduce the voltage noise level on the output since the output of this module will be connected to the high voltage amplifier, the voltage noise will be magnified by the gain value of the high voltage amplifier and this magnified noise can reduce the precision of the tip location in three axes. Additionally, the low pass filter can avoid the first fundamental resonance frequency of the piezoelectric tube to avoid unwanted oscillation during the experiments. The general specifications of the module are as follows:

- Differential or single-ended signals on all of the inputs.
- Ultra-low noise linear voltage regulators on the power lines.
- Ultra-low noise and drift +10 and -10 volts reference for the offsets.
- Adjustable minimum and maximum voltage for the low pass filter to limit the output voltage (to avoid damaging the piezo).

- 7^{th} and 8^{th} order low pass filter to reduce the noise and cut the sharp edges of the scanning waveform. The cutoff frequency and the topology of the low-pass filtered can be designed and implemented as per the requirements of the project.
- The offsets and the attenuation coefficient are controlled by a computer in 256 steps (LabVIEW or other languages).
- The maximum bandwidth of the attenuators is 500 kHz. If higher bandwidth is required, a regular potentiometer can be installed.

Since the requirements for X and Y directions are almost identical, the X and Y modules are identical in terms of the circuit board, but the filters and coefficients can be tuned separately. It is possible to set up each module in two different modes, which are shown in Figures 2.11a and 2.11b. The functionality of the first mode is as follows. There are two external inputs with the capability of accepting differential and single-ended signals. Then the input signals can be magnified by a constant coefficient (the minimum coefficient value can be one) and then there is a voltage divider on the path of “In 1” input. So, the scanning waveform from the main controller can be connected to this input and will be divided by the desired value. There is a dedicated output connection named “out 1” for this signal. The second input can be used as a separate offset signal from the controller or in case of any modulation in X and Y directions, the modulation signal can be connected here. There is also a digitally controlled offset value which is generated internally. The value can be tuned by the operator or the main controller software in case of integration of this module with the controller. Then the three signals go to the voltage adder amplifier and the output is passed through an eighth-order low-pass filter for the aforementioned purposes. The final output is accessible on the “Out 2” connector. In the second mode, the sequence of the operations is different as it can add the two input signals after the magnification and pass it through the voltage divider. Thus, this mode can reach gains lower than one for the two inputs. This mode can be more helpful for applications with small modulations in the X-Y plane.

The next part is the Z module, which has four modes and each of them is configurable as per the requirements of the project. Compared to the XY modules, this module has more functionality and extra functionality usually comes with more complexity. The four working modes are shown in Figure 2.12. One additional input is considered for the Z module compared to the X and Y modules in the case of different kinds of modulation. Thus there are three inputs for external signals either differential or single-ended and two single-ended outputs. The first mode (Figure 2.12a) is very

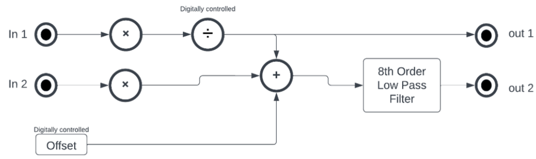

(a)

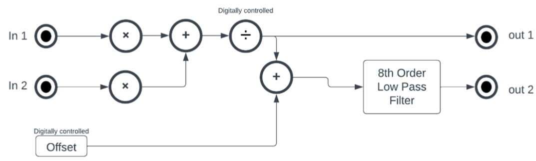

(b)

Figure 2.11: Simple schematic for the X, and Y modules for a) first mode, b) second mode

similar to the first mode of the X-Y module, except for the fact that there is one more input "In 3" and the signal can be multiplied and added to the output of the low pass filter. The summation signal is connected to "out 2". As described, the third input can get bypassed from the low pass filter and it can be beneficial for modulations with a frequency higher than the cutoff frequency of the filter. This can avoid any phase shift and change in modulation amplitude. The second mode (Figure 2.12b) is similar to the X-Y second mode and we can apply division on the summation signal of inputs one and two. The third input works as it was described above. For the third and fourth modes (Figures 2.12c and 2.12d), the third input is added to the other signals and the result is passed onto the low-pass filter. If the modulation frequency of the modulation is lower than the cutoff frequency of the filter, these modes can be useful. The difference between the third and fourth modes is the ability of signal division on "In 2", as it was discussed above. Choosing the best working mode depends on the experimental requirements and many other design parameters like the modulation frequency, amplitude, low-pass filter frequency, low-pass filter topology, resonance frequency of the system, etc.

Abs, Log, PID with a Low-pass filter

The tunneling current can flow in two directions depending on the polarity of the tunneling bias, thus positive and negative signals are possible on the output of the pre-amplifier. The opposite directions for negative and positive signals can cause trouble for the feedback loop. There are two solutions for this. First: flipping the signs of the tunneling setpoint and changing the polarity of the output signal of the

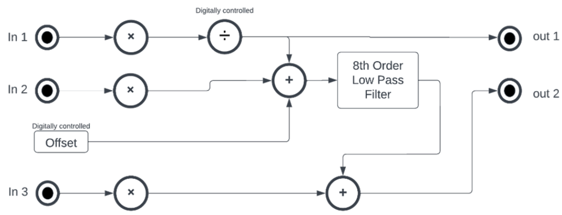

(a)

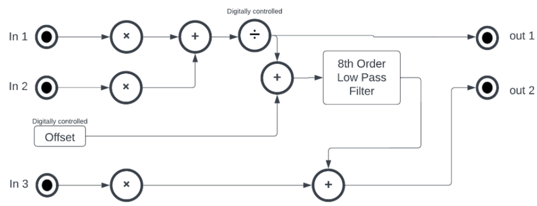

(b)

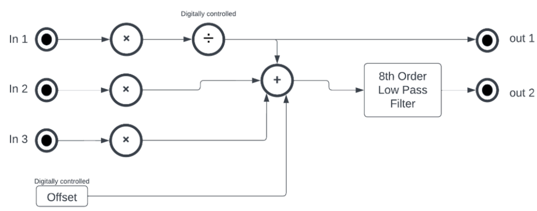

(c)

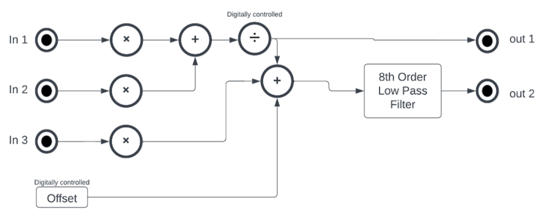

(d)

Figure 2.12: Simple schematic of the Z module for the a) first mode, b) second mode, c) third mode, d) fourth mode.

feedback. This solution can get rather challenging in the case of the need for changing the bias voltage during the scan time because all the parameters should be changed with a specific timing to avoid tip crashes or losing the tunneling current. The second solution is applying an absolute value operator on the input signal (output of the pre-amplifier). This avoids the aforementioned issue with the polarity and the feedback loop can work without any problems. It also reduces the complexity of changing the tunneling bias and having stable control over the tip location. Thus, the next required module is an absolute amplifier. A simple schematic is shown in Figure 2.13a. The output of this module can be internally connected to the input of the logarithmic amplifier and there are two external outputs. "Out 1" is directly connected to the absolute amplifier and "Out 2" is a buffered signal of the input and it can deliver up to 250 mA.

Since the tunneling current magnitude is an exponential function of the tip-sample distance, having a logarithmic amplifier is a must. As shown in Figure 2.13b, there are two inputs for this module, one is internal and comes from the absolute amplifier and the other one is for an external signal. The logarithmic amp can perform logarithm operations over 8 decades (very wide dynamic range). The output range in the standard configuration is ±10 volts. "Out 1" is the connector for the external connection and the second output can be connected internally to the PID module.

Figure 2.13c shows the PID module with the integrated low-pass filter. This module has three inputs, one internal and two external connectors. The internal input can be disconnected and leaves room for the external inputs. The two external inputs can be used as the PID setpoint and input for the main feedback signal. There is also the possibility of adjusting the setpoint internally, which can be controlled digitally by the software. After the voltage adder, the error signal goes through the PID controller. The PID coefficients are controlled by the computer in 256 steps (LabVIEW or other language). The maximum values for each gain can be tuned by choosing the appropriate resistors and capacitors values. One active low pass filter with a tunable cutoff frequency is placed after the PID controller to limit the bandwidth and avoid oscillations caused by the white noise and slight tip crashes during the scan time. Just before the output connector, there is an inverter to invert the polarity of the PID. This can be bypassed due to the next module and its configuration.

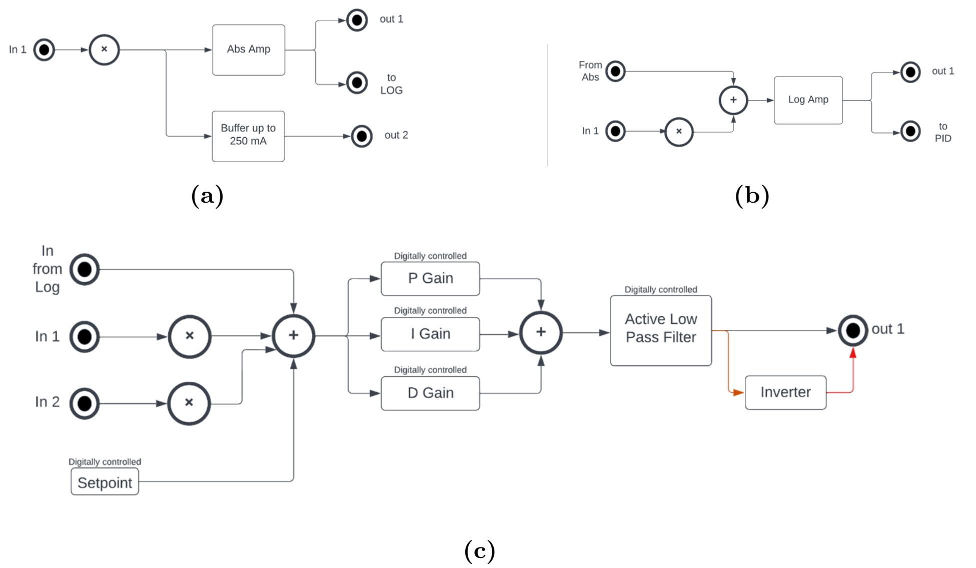

Figure 2.13: Simple schematic for the a) absolute amplifier, b) logarithmic amplifier, c) PID with a low-pass filter

2.2.4 Mechanical design

There are many different mechanical designs for the SPM which were introduced thoroughly in the literature[15]. EC-STM has some specific challenges and these should be considered during the design steps. The main considerations are as follows:

- The sample should always placed horizontally and the tip should land on the sample from the top since the surface should be in contact with the electrolyte.
- The electrolytes can be very corrosive and damaging to the mechanical parts. Protective properties are essential.
- The electrolyte should be in contact with as few parts as possible since the cleanliness of the entire electrochemical cell is crucial and those parts should be resistive against the electrolytes and do not contribute to the electrochemical reactions inside the cell.
- Easy and fast assembling steps for the experiments because the complexity of these steps can lead to introducing extra contamination to the sample surface and the electrochemical cell.

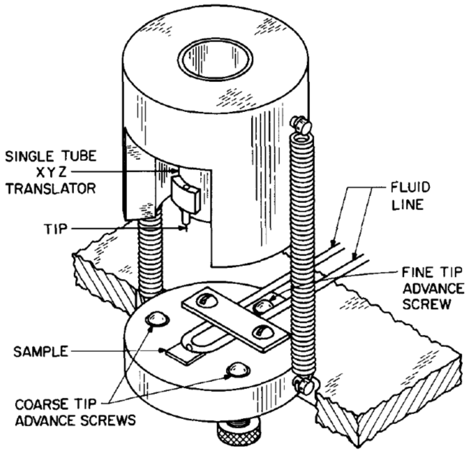

Figure 2.14: STM design which operates with a drop of fluid on the sample. The two springs hold the top piece, which has the scanner tube, and hold the tip in an upside-down configuration. Two coarse advance screws are deployed to be adjusted by hand for the initial approaching step and one fine screw is connected to the motor to adjust the height automatically during the auto approach step[17]. Reprinted with permission from Elsevier.

The best fit for these requirements is the single-tube scanning tunneling microscope design. In this design[17], the single tube scanner head is placed on the top of the sample and secured with springs. The tip is hanging on the single tube translator (scanner head) and it can land vertically on the sample. The sample and the entire electrochemical setup can be installed on the base plate. By removing the single tube transducer, the operator has enough room to assemble the sample and EC cell quickly. Three fine screws help the coarse approach steps and the fine approach step can be done by the accurate motors.

Figure 2.15a shows the designed base plate. This is the main plate that holds the EC cell, the sample, the scanner head, and fine screws/motors. This plate is connected to a vibration isolation system from three points which are shown with white signs with three metallic pillars. In the center, there is a large circular cut that accommodates the EC cell and sample. The three cyan-colored cylinders show the locations of the motors and the four arrows can be seen pointing downwards. These arrows show the direction of the forces applied to this plate. The center arrow is coming from the center of mass of the plate and the three outer are related to the forces on the three fine screws/motors holding the scanner head. The chosen material for this part is Invar to reduce thermal drifts in the XYZ direction. To ensure the rigidity of the design, a finite element simulation can shed some light on the design characteristics. The result shows that the first fundamental resonance frequency is 7727.52 Hz which is high enough for many experiments.

The next part is the scanner holder that is shown in Figure 2.15b. Three seats are designed at the bottom (indicated with white signs) to land on the upward fine screws to hold the scanner head assembly (scanner holder + piezo tube). On the top part, the indicated cyan area is the plane that the piezo tube can be attached and the arrow shows the direction of the force on this part from the piezo tube. The desired material for this part is Invar as well. The first resonance frequency of this part is 7599.42 Hz, according to the simulation.

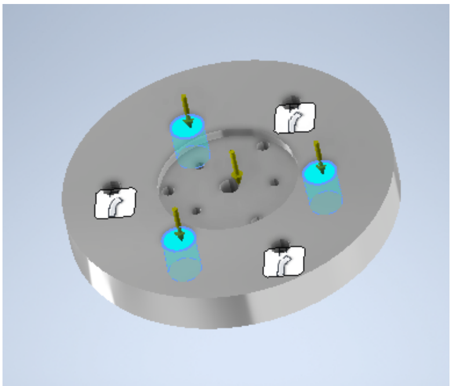

(a)

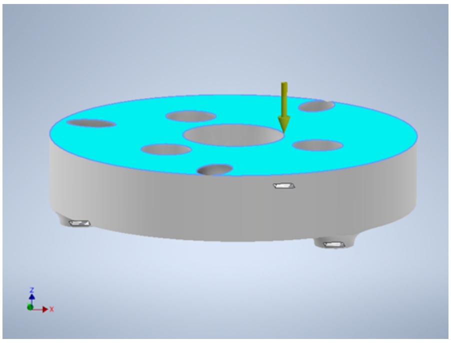

(b)

Figure 2.15: a) The base plate with the three white signs shows the location of the three main legs that hold the entire microscope. The three cyan-colored cylinders show the locations of the motors and the arrows indicate the directions of forces on this plate. The center arrow is the result of the mass of this plate and the three surrounding arrows show where the three fine screws/motors hold the mass of the scanner head. b) The scanner holder which has three seats for the fine screws indicated with white signs. The cyan surface shows the plane that the piezo tube can get connected to and the arrow shows the force direction caused by the mass of the piezo tube.

The electrochemical cell, which will be filled with an electrolyte during the experiments, is an important part of the setup. The design of this part needs more sophisticated computational fluid dynamic simulations to improve the properties of the cell. Appendix A is dedicated to the design for this part. The cross-section of the design in the Y-Z plane crossing the center of the sample is shown in Figure 2.16. The EC cell is in yellow and the insulator plate is in blue. The base plate is located at the bottom and the tip (in green) is hanging from the tip holder. The selected material for

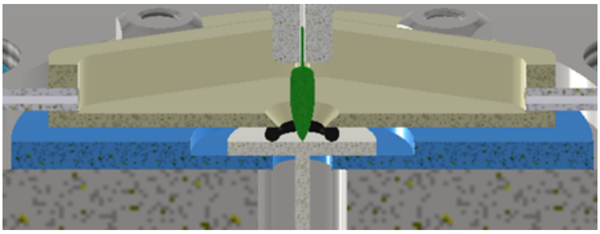

Figure 2.16: Cross section of the design in Y-Z plane. The EC cell is in yellow and the insulator plate is in blue. The base plate is located at the bottom and the tip (in green) is hanging from the tip holder. The O-ring in black is located above the sample and underneath the EC cell to avoid electrolyte leakage and the inlet and outlet are located on the left and right side of the EC cell.

the tip holder, the EC cell, and the insulator plate is PEEK since PEEK is a very good electrochemically resilient material for basic and acidic electrolytes and it is suitable for a large spectrum of electrochemical experiments. PEEK is also resilient against the conventional cleaning procedure of cleaning (soaking in potassium permanganate, then diluted piranha solution, and several times boiling in milli-Q water). The O-ring in black is located above the sample and underneath the EC cell to avoid electrolyte leakage and the inlet and outlet are located on the left and right side of the EC cell. The cell can be fixed to the base plate by three nuts and the tightness of the nuts will indicate the total force on the O-ring and the sample. Extra force can be damaging for soft samples like gold, so precautions should be taken.

The entire CAD design is depicted in Figure 2.17a, which shows the location of the three motors under the base plate in gray, the reference electrode secured on the base plate in yellow, and the scanner head assembly on the top. By having the designed parts manufactured, the assembling process was done and Figure 2.17b shows the final result. The three motors are located below the main plate and secured tightly to it. The whole scanner head assembly is located on the three motors and can lift and lower the head for a coarse approach and auto-approach mechanism. There are two thin pipes on both sides of the main plates which are connected to the EC cell. Pumping the electrolyte in and out is possible through these pipes. Since the scanner holder is detachable from the piezo tube, it is easy to have different piezo tubes for different experiments. The longer scanner head in Figure 2.17c provides a larger scan area. In this figure, all the electrical connections are shown and the inlet and outlet pipes are connected as well.

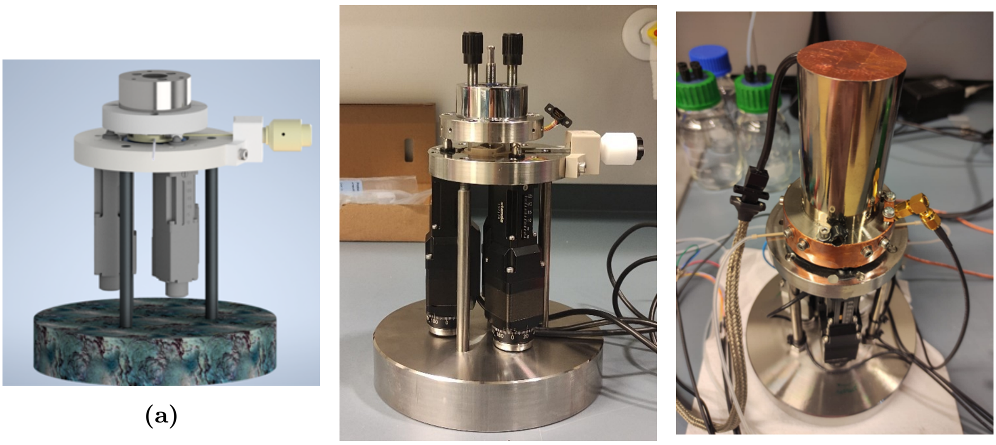

(a) (b) (c)

Figure 2.17: a) The CAD model of EC-STM design b) manufactured and assembled with a smaller piezo tube, c) with a piezo tube for larger scan areas.